Hindawi
Complexity
Volume 2021, Article ID 1957510, 9 pages
https://doi.org/10.1155/2021/1957510

*Research Article*

# Adaptive Super-Twisting Sliding Mode Control of Permanent Magnet Synchronous Motor

**Chao Lu and Jing Yuan**

*School of Information Engineering, Suqian University, Suqian 223800, China*

Correspondence should be addressed to Chao Lu; lchao@sqc.edu.cn

Received 29 June 2021; Revised 2 August 2021; Accepted 17 August 2021; Published 31 August 2021

Academic Editor: Xiaodi Li



The work has developed an innovative speed loop controller for the permanent magnet synchronous motor (PMSM) system. The main advantage of the presented method lies in the fact that the boundary of the lumped disturbance is not required. Under this case, the severe chattering caused by the inappropriate choice of parameters can be avoided. Finally, the simulation and experimental consequences are given to demonstrate the efficiency of the proposed algorithm used to control a PMSM system subject to the lumped disturbance.

## 1. Introduction

Owing to its superiorities of high control precision, high energy conversion rate, and low rotor inertia, permanent magnet synchronous motor (PMSM) has been applied to numerous fields, such as aerospace, new energy vehicle, industrial robot, and so on [1–3]. Nowadays, in actual industrial applications, the control strategies of the PMSM speed regulation system mostly adopt a classical proportional-integral (PI) controller. It is noted that the structure of such a controller is uncomplicated, and its parameters are easy to be modified [4, 5]. Nevertheless, the scheme for PI is a linear method. With the system running for a long time and emerging external disturbances, the system parameters will fluctuate nonlinearly. Therefore, the strategy based on PI cannot meet the qualifications of high performance of the servo system.

In order to settle the defects of the traditional PI controller, the nonlinear control plans are employed in the speed controller. With the evolution of control technologies, multifarious nonlinear control algorithms have been presented by scholars. Abundant schemes are feasible in the PMSM servo system among them, such as fuzzy control [6, 7], adaptive control [8, 9], fractional-order control [10, 11], disturbance observer [12–14], sliding mode control (SMC) [15, 16], intelligent control [17–19], and so on. By applying these algorithms to PMSM servo systems, the performances of PMSM servo systems have been noteworthily improved.

Among the aforementioned algorithms, the SMC method, which can guarantee excellent tracking performance despite parameters or model uncertainties, has been widely used in nonlinear systems owing to its strong robustness and fast dynamic response [20, 21]. Nonetheless, the chattering phenomenon is the main factor that hinders the further development of SMC. To cripple the chattering effect, different methods have been adopted, which can be summarized as the following three types [22–24]:

(i) The discontinuous control functions are substituted by "saturation" or "sigmoid ones."

(ii) The higher-order SMC techniques are used.

(iii) The controllers with dynamical gains are utilized.

By adopting these ideas, the modified SMC approaches have been successfully applied in many fields. Feng et al. [25] proposed a new reaching law, which achieved the expected goal of impairing chattering. The author in [26] used a super-twisting algorithm as the loop of the speed controller to fulfill high performance and attenuate

chattering. In [27], an adaptive first-order sliding mode controller was proposed and evaluated for the control of an electro-pneumatic actuator. However, the above research studies neglect the problem of uncertainty boundary which determines the choice of control parameters. In order to solve the aforementioned problem, the authors in [28, 29], respectively, proposed adaptive sliding mode plans. In [28], the boundary of disturbance is required in advance, and the adoption of a low-pass filter brings about some disadvantages such as time delay. In [29], the gain may be large, which leads to chattering. Everything has two sides, and these articles have own advantages and disadvantages. However, to some extent, they have promoted the development of control technology.

Motivated by the aforementioned observations, the main work of this paper concentrates on the design of the speed controller. The main contributions are outlined as follows. By combining the super-twisting algorithm and the adaptive technique, a novel speed loop controller is developed such that the requirements for the high performance of the PMSM servo system are satisfied. Particularly, the super-twisting algorithm can make the motor have superior starting characteristics and reduce the chattering effect. Also, the adaptive law can effectively handle the issue that the disturbance boundary cannot be obtained beforehand.

The remainder of the paper is organized as follows. In Section 2, the traditional model of surface-mounted PMSM is introduced, and the model uncertainties are analyzed. In Section 3, the design of the proposed ASMC controller and its stability analysis are presented. In Section 4, simulation and experimental results are shown to demonstrate the effectiveness of the proposed control strategy. The conclusions are drawn in Section 5.

## 2. Preliminaries

In this section, to facilitate the proposal of the new method, some preliminaries are introduced, including PMSM models and basic perturbation boundary analysis.

*2.1. Model of PMSM System.* In order to establish the mathematical model of surface-mounted PMSM in the coordinate system, it should be required to make the following assumptions:

(a) The saturation of the motor core is ignored.

(b) The eddy current and hysteresis loss in the motor are excluded.

(c) The current of the motor is a symmetrical three-phase sine wave current.

Based on the above three assumptions, the surface-mounted PMSM mathematical model in the rotor speed coordinate system is expressed as follows [30]:

$$\begin{cases} L_s \dfrac{\mathrm{d}i_d}{\mathrm{d}t} = -Ri_d + P_n L_s \omega i_q + U_d, \\ L_s \dfrac{\mathrm{d}i_q}{\mathrm{d}t} = -Ri_q - P_n L_s \omega i_d + U_q - P_n \varphi_f \omega, \\ J \dfrac{\mathrm{d}\omega}{\mathrm{d}t} = -B\omega + 1.5 P_n \varphi_f i_q - T_L. \end{cases} \tag{1}$$

To carry out the static decoupling of the axis current, we usually make $i_d$ equivalent to 0, since the magnetic flux is completely offered by the permanent magnet when $i_d = 0$. The current on the straight axis is 0, which makes the motor be without armature reaction of the straight axis (i.e., the straight axis does not contribute torque). All the current of the motor is used to obtain electromagnetic torque, which is equivalent to a separately excited DC motor. Only by controlling the value, the torque of the motor can be controlled, which naturally realizes the static state of the motor decoupling. Consequently, the mathematical model of the motor can be simplified as

$$\begin{cases} L_s \dfrac{\mathrm{d}i_q}{\mathrm{d}t} = -Ri_q + U_q - P_n \varphi_f \omega, \\ J \dfrac{\mathrm{d}\omega}{\mathrm{d}t} = -B\omega + 1.5 P_n \varphi_f i_q - T_L, \end{cases} \tag{2}$$

where $i_q$ and $i_d$ represent the current component of the motor stator current on the $d$ and $q$ axes, respectively; $U_d$ is the stator $d$-axis voltage and $U_q$ is the stator $q$-axis voltage; $T_L$ is the load torque; $J$ is the rotational inertia; $\omega$ is the mechanical angular velocity of the motor; $B$ is friction coefficient; $\varphi_f$ is the motor flux linkage; and $P_n$ represents motor pole pairs.

By formula (2), the relationship between angular velocity $\omega$ and $i_q$ is as follows:

$$\dot{\omega} = -\frac{B}{J}\omega + \frac{1.5 P_n \varphi_f}{J} i_q^* + d_0(t), \tag{3}$$

where $i_q^*$ is the reference current of $q$ axis and $d_0(t) = -(T_L/J) - ((1.5 P_n \varphi_f)/J)(i_q^* - i_q)$ can be considered as the lumped disturbance.

*2.2. Analysis of Lumped Disturbance Boundary.* PMSM speed control is essentially the tracking problem of the actual servo system output signals and the given reference signals. As a result, the speed error is defined as

$$\sigma = \omega - \omega_r, \tag{4}$$

where $\omega_r$ is given reference mechanical angular velocity. Differentiating (4) yields

$$\dot{\sigma} = \dot{\omega} - \dot{\omega}_r\,. \tag{5}$$

Substituting (2) in the above equation produces

$$\dot{\sigma} = -\frac{B}{J}\sigma + d(t) + \frac{1.5P_n\varphi_f}{J}i_q^*, \tag{6}$$

where $k_t = 1.5P_n\varphi_f$ is the torque constant and $d(t) = -(T_L/J) - (k_t/J)(i_q^* - i_q) - (B/J)\omega_r$.

Although the mathematical model established only takes into account the external load disturbance mentioned in Section 2.1, it is usually accompanied by the parameter variation during the motor operation. Considering various disturbance, the motor model is further improved as

$$\dot{\sigma} = \left(-\frac{B}{J}\sigma + d(t) + \Delta\varpi\right) + \left(\frac{1.5P_n\varphi_f}{J} + \Delta\rho\right)i_q^*. \tag{7}$$

Then, we denote $\varpi_0(x,t) = -(B/J)\sigma + d(t)$, $\rho_0(x,t) = (k_t\varphi_f/J)$, where $\Delta\varpi$ is the sum of parameter variables and load disturbances and $\Delta\rho$ is the parameter variable. Considering that the change of parameter variable is smaller in comparison with the change of parameter itself, it is assumed that

$$\frac{|\Delta\rho(x,t)|}{\rho_0(x,t)} = \xi(x,t) \le \xi_1 < 1, \tag{8}$$

where $\xi_1$ is a constant of bounded but unknown value. In addition, we assume $|\varpi_0(x,t)| \le \delta_1|\sigma|^{1/2}$. Meanwhile, $\Delta\varpi$ is not a pulse signal, that is to say,

$$|\Delta\dot{\varpi}(x,t)| \le \delta_2, \tag{9}$$

where $\delta_2, \delta_2$ are random positive numbers, but their values are unknown.

After meeting the above hypothesis, (6) can be rewritten in the following form:

$$\dot{\sigma} = \varpi_0(x,t) + \Delta\varpi + \underbrace{\left(1 + \frac{\Delta\rho(x,t)}{\rho_0(x,t)}\right)}_{\rho_1(x,t)}u, \tag{10}$$

where $u = \rho_0(x,t)i_q$.

From (7), it is derived that

$$1 - \xi_1 \le \rho_1(x,t) \le 1 + \xi_1. \tag{11}$$

## 3. Structure of Speed Controller

In general, PMSM adopts the scheme of magnetic field orientation control (FOC), where the system is a double closed-loop structure. The sliding mode controller is a speed loop designed outside the PMSM system. In this part, the super-twisting controller is firstly designed. Then, the adaptive law is applied to the designed super-twisting controller.

*3.1. Designing Super-Twisting Controller.* By using high-order sliding mode related theory, the following super-twisting controller is given:

$$u = -\lambda_m\sqrt{|\sigma|}\,\mathrm{sign}(\sigma) - \int\frac{u_1}{2}\,\mathrm{sign}(\sigma)\mathrm{d}\tau, \tag{12}$$

where $\lambda_m$ and $u_1$ are gains of the controller.

Since it is difficult to obtain the precise information about boundary, we usually assume that the lumped disturbance is bounded. However, the gains of the super-twisting controller depend on the upper and lower values of the boundary in the process of experiment. In order to solve this problem, we firstly need to prove that the lumped disturbance is bound at the mathematical level.

Therefore, we denote $u_* = \Delta\rho(x,t) + \rho_1 v$. Taking the derivative of $u_*$, one can obtain

$$\dot{u}_* = -\frac{u_1\rho_1(x,t)}{2}\mathrm{sign}(\sigma) + \Delta\dot{\varpi} + \dot{\rho}_1\, v, \tag{13}$$

where $\dot{v} = -(u_1/2)\mathrm{sign}(\sigma)$.

Additionally, $\varepsilon_{\lambda_m}$ and $\varepsilon_{u_1}$, respectively, represent their borders. There exist constant parameters $\varepsilon_\lambda$ and $\varepsilon_{u_1}$ such that $\varepsilon_\lambda = \lambda_m - \lambda_m^* < 0$ and $\varepsilon_{u_1} = u_1 - u_1^* < 0$. Then, it is not difficult for us to deduce

$$\left|\dot{\rho}_1(x,t)v\right| \le \frac{\dot{\rho}_1(x,t)}{2}\int_t^0 u_1\mathrm{d}\tau \le \frac{\dot{\rho}_1(x,t)}{2}u_1^* t \le \delta_3, \tag{14}$$

where $\delta_3 > 0$ is a constant of bounded but unknown value. Based on the above analysis, it is easy to obtain the lumped disturbance of the system as follows:

$$|\dot{\psi}(x,t)| = \Delta\dot{\varpi}\,(x,t) + \dot{\rho}_1(x,t)v \le \delta_2 + \delta_3 = \delta_4, \tag{15}$$

where $\delta_4$ is unknown positive number and $\psi(x,t)$ is the lumped disturbance.

So far, we do not know the boundary value of each disturbance, but they have satisfied the bound for all possible disturbances. Therefore, the problem is simplified to the design of adaptive law such that the sliding variables $\sigma \longrightarrow 0$ and $\dot{\sigma} \longrightarrow 0$ are satisfied in finite time in the case of unknown boundary value.

*3.2. Main Results.* In general, the controller gains will be selected in very large values to improve the robustness of the system, but this leads to chattering of the system, which is not tolerated in some systems. In order to solve this problem, the adaptive law method can be used to dynamically adjust the controller gain online. According to the relevant theory, the designed adaptive law is formulated in the following theorem.

**Theorem 1.** *For a positive constant $\lambda_M$, when $\lambda_m \le \lambda_M$, $\dot{\lambda}_m = \eta, \dot{u}_1 \ge 2\varepsilon\eta$; when $\lambda_m > \lambda_M$,*

$$\begin{aligned}\dot{\lambda}_m &= \phi\sqrt{\frac{\gamma}{2}}\mathrm{sign}(|\sigma| - \mu),\\ \dot{u}_1 &\ge 2\varepsilon\phi\sqrt{\frac{\gamma}{2}}\mathrm{sign}(|\sigma| - \mu).\end{aligned} \tag{16}$$

*Proof.*

$$\begin{bmatrix} \dfrac{\mathrm{d}\left(|\sigma|^{1/2}\mathrm{sign}(\sigma)\right)}{\mathrm{d}t} \\ \\ \dot{u}_* \end{bmatrix} = \frac{1}{\left||2\sigma|^{1/2}\mathrm{sign}(\sigma)\right|} \begin{bmatrix} -\lambda_m\rho_1|\sigma|^{1/2}\mathrm{sign}(\sigma) + u_* + \varpi_1 \\ \\ -\dfrac{u_1\rho_1}{2|\sigma|^{1/2}\mathrm{sign}(\sigma)}|\sigma|^{1/2}\mathrm{sign}(\sigma) + \dot{\chi}(x,t) \end{bmatrix}$$

$$= \frac{1}{2|\sigma|^{1/2}\mathrm{sign}(\sigma)} \begin{bmatrix} -ab_1 & 1 \\ \\ -\beta b_1 & 0 \end{bmatrix} \begin{bmatrix} |\sigma|^{1/2}\mathrm{sign}(\sigma) & \\ \\ \omega_* & \omega_* \end{bmatrix} \tag{17}$$

$$+ \frac{1}{2|\sigma|^{1/2}\mathrm{sign}(\sigma)} \begin{bmatrix} 1 & 0 \\ \\ 0 & 2|\sigma|^{1/2}\mathrm{sign}(\sigma) \end{bmatrix} \begin{bmatrix} a_1 \\ \\ \dot{\chi}(x,t) \end{bmatrix}.$$

Based on the above analysis, we know that

$$\varpi_0 = t_1|\sigma|^{1/2}\mathrm{sign}(\sigma),$$

$$\dot{\chi}(x,t) = \frac{t_2}{2}\frac{|\sigma|^{1/2}\mathrm{sign}(\sigma)}{\left||\sigma|^{1/2}\mathrm{sign}(\sigma)\right|}, \tag{18}$$

where $t_1 = (0, \delta_1], t_2 = (0, \delta_2]$.

Then, in view of (17), (16) can be rewritten as

$$\begin{bmatrix} \dfrac{\mathrm{d}\left(|\sigma|^{1/2}\mathrm{sign}(\sigma)\right)}{\mathrm{d}t} \\ \\ \dot{u}_* \end{bmatrix} = \frac{1}{\left||2\sigma|^{1/2}\mathrm{sign}(\sigma)\right|} \begin{bmatrix} -(\lambda_m\rho_1 - t_1) & 1 \\ \\ -(u_1\rho_1 - t_2) & 0 \end{bmatrix} \begin{bmatrix} |\sigma|^{1/2}\mathrm{sign}(\sigma) \\ \\ \omega_* \end{bmatrix}. \tag{19}$$

For the convenience of expression, we denote $\begin{bmatrix} \zeta_1 \\ \zeta_2 \end{bmatrix} = \begin{bmatrix} |\sigma|^{1/2}\mathrm{sign}(\sigma) \\ u_* \end{bmatrix}$. To prove the stability of the system, we consider the following Lyapunov function:

$$V(\zeta_1, \zeta_2, \lambda_m, u_1) = V_0 + \frac{1}{2\xi_1}(\lambda_m - \lambda_m^*)^2 + \frac{1}{2\xi_2}(u_1 - u_1^*)^2, \tag{20}$$

where

$$V_0(\zeta) = \left(\lambda + 4\varepsilon^2\right)\zeta_1^2 + \zeta_1^2 - 4\varepsilon\zeta_1\zeta_2 = \zeta^T P\zeta, \tag{21}$$

$$P = \begin{bmatrix} \lambda + 4\varepsilon^2 & -2\varepsilon \\ -2\varepsilon & 1 \end{bmatrix}, \quad \varepsilon > 0. \tag{22}$$

Obviously, the matrix $P$ is positive definite matrix when the parameter $\lambda$ is greater than 0. By taking the derivative of $V_0(\zeta)$ in (20), one can derive

$$\dot{V}_0(\zeta) = \dot{\zeta}^T P\zeta + \zeta^T P\dot{\zeta} \le \zeta^T \widetilde{Q}\zeta. \tag{23}$$

To stabilize the system, the symmetric matrix $Q$ must be positive definite. Hence, the characteristic value of matrix $Q$ needs to be greater than 0. Hence, we enforce

$$u_1 = 2\varepsilon\lambda_m. \tag{24}$$

In view of (22), it is easy to show that

$$V_0(z) \le -rV_0^{1/2}(z), \tag{25}$$

where

$$r = \frac{\varepsilon\lambda_{\min^{1/2}}(P)}{\lambda_{\max}(P)}. \tag{26}$$

Based on the finite-time Lyapunov stability theorem, taking the derivative of $V(\zeta_1, \zeta_2, \lambda_m, u_1)$ in (19) gives

$$\begin{aligned}\dot{V}(\zeta,\lambda_m,u_1) &= \dot{\zeta}P\zeta + \zeta^T P\dot{\zeta} + \frac{1}{\gamma_1}\varepsilon_{\lambda_m}\dot{\lambda}_m + \frac{1}{\gamma_2}\varepsilon_{u_1}\dot{u}_1 \\ &\le -\frac{1}{|\zeta_1|}\zeta^T\tilde{Q}\zeta + \frac{1}{\gamma_1}\varepsilon_n\lambda_m + \frac{1}{\gamma_2}\varepsilon_{u_1}\dot{u}_1 \\ &\le -rV_0^{1/2} + \frac{1}{\gamma_1}\varepsilon_{\lambda_m}\dot{\lambda}_m + \frac{1}{\gamma_2}\varepsilon_{u_1}\dot{u}_1 \\ &= -rV_0^{1/2} - \frac{\phi_1}{\sqrt{2\gamma_1}}\left|\varepsilon_{\lambda_m}\right| - \frac{\phi_2}{\sqrt{2\gamma_2}}\left|\varepsilon_{4_1}\right| \\ &\quad + \frac{1}{\gamma_1}\varepsilon_{2_m}\dot{\lambda}_m + \frac{1}{\gamma_2}\varepsilon_{u_1}\dot{u}_1 + \frac{\phi_1}{\sqrt{2\gamma_1}}\left|\varepsilon_{n_m}\right| + \frac{\phi_2}{\sqrt{2\gamma_2}}\left|\varepsilon_{u_1}\right| \\ &\le -\eta_0\sqrt{V(\zeta_1,\zeta_2,\lambda_m,u_1)} + \frac{1}{\gamma_1}\varepsilon_{\lambda_m}\dot{\lambda}_m \\ &\quad + \frac{1}{\gamma_2}\varepsilon_{u_1}\dot{u}_1 + \frac{\phi_1}{\sqrt{2\gamma_1}}\left|\varepsilon_{\lambda_m}\right| + \frac{\phi_2}{\sqrt{2\gamma_2}}\left|\varepsilon_{u_1}\right| \\ &\le -\eta_0\sqrt{V(\zeta_1,\zeta_2,\lambda_m,u_1)}.\end{aligned} \tag{27}$$

The proof of Theorem 1 is completed. □

*Remark 1.* It is worth pointing out that the proposed scheme is concluded as follows. Firstly, we introduce the model of surface-mounted PMSM, and the model uncertainties are analyzed. Secondly, the proposed ASMC controller design is proposed. Under the developed controller, the stability of the closed-loop system is guaranteed. Finally, the simulation and experimental results are given to confirm the feasibility of the proposed control strategy.

## 4. Simulation and Experimental Results

*4.1. Simulation Results.* In order to validate the effectiveness of the proposed scheme, a group of comparative simulations of speed loop controllers is performed in Matlab-Simulink 2013b environments by, respectively, using PI, STW, and ASTW algorithms. The simulation and experiment parameters of PMSM are listed in Table 1.

The parameters of current loop PI controller are consistent. The proportional gain is $k_p = 10$, and the integral gain is $k_i = 0.1$. The system reference speed is given as 600 rpm. The load torque $T_l = 1.65$ N is suddenly added to the PMSM system at 0.1 s and abruptly removed from the system at 0.2 s. The parameters of the proposed speed controller are $\phi = 1, \gamma = 2, \mu = 0.001, \varepsilon = 250, \eta = 10000$, and $\lambda_M = 5$.

The speed waveforms of the three methods from 0 to 600 rpm are shown in Figure 1. It can be observed from Figure 1 that the PI has a very short rise time but a very large overshoot compared with the other two controllers. The rise time and adjusting time of ASTW are a little shorter compared with the STW method. Simulation results of anti-load disturbance of the three controllers are shown in Figure 2. When the same load torque is suddenly added or removed from the system at the same time, the fluctuation of speed of the system under the ASTW method is the smallest, and the recovering time against disturbance is the shortest. Additionally, the response of motor $q$ axial current, load torque, and phase current in the presence of a sudden disturbance load is, respectively, shown in Figures 3 and 4. One can see that the starting current of motor under ASTW is the smallest. Meanwhile, the chattering has been attenuated for the ASTW algorithm. A comparison of performance indices on the three methods is shown in Table 2. Moreover, the comparisons of the $d$-axis current responses and the $T_L$ under the three controllers are, respectively, shown in Figures 5 and 6.

Table 1: Main parameters of PMSM.

| Quantity | Symbol | Value and unit |
|---|---|---|
| Stator flux linkage | $\varphi_f$ | 0.1068 wb |
| Stator resistance | $R$ | 0.925 Ω |
| Moment of inertia | $J$ | 0.1068 kg/m$^2$ |
| Torque constant | $K_t$ | 0.641 Nm/A |
| Number of pole pairs | $P_n$ | 4 |

*4.2. Experimental Results.* The core equipment of PMSM servo system mainly consists of the PMSM control board, permanent magnet synchronous motor drive board, orthogonal encoder, signal acquisition device, magnetic powder brake, permanent magnet synchronous motor, and so on. The control board of the experimental platform uses DSP TMS320F28335 as the main control chip, and the experimental program is written in a mixture of C language and assembly language. The permanent magnet synchronous motor of the experimental platform is driven by IPM three-phase voltage source inverter. The IPM module of the experimental platform adopts PS21865-AP chip produced by Mitsubishi Corporation of Japan. The collection of experimental data can be completed by using oscilloscope.

Similarly, the current values of different algorithms are the same in order to guarantee the fairness of the experiment, i.e., the proportional gains are $k_p = 0.2$ and the integral gains are $k_p = 0.04$. The experimental parameters of the proposed speed controller are $\phi = 1, \gamma = 0.1, \mu = 0.05$, $\varepsilon = 5, \eta = 500$, and $\lambda_M = 0.1$.

Figure 7 shows the speed waveform diagram at startup phase under different algorithms. It reveals that the overshoot time, adjusting time, and the rise time in ASTW are all shortest compared with the other algorithms. Figure 8 shows the experimental results of PI, STW, and ASTW with load torque disturbance at 600 rpm. It shows that the maximum speed drop of ASTW, which is almost 10 rpm, is the smallest. Meanwhile, the speed of ASTW can return to reference in the shortest time. In Figures 9–11, each image contains three subimages. The three subimages are PI, STW, and ASTW from top to bottom, respectively. Figure 9 is the response of q-axis current in the startup phase and with load, and Figure 10 is the response of d-axis current in the startup phase and with load. Figure 11 is comparison of the phase current

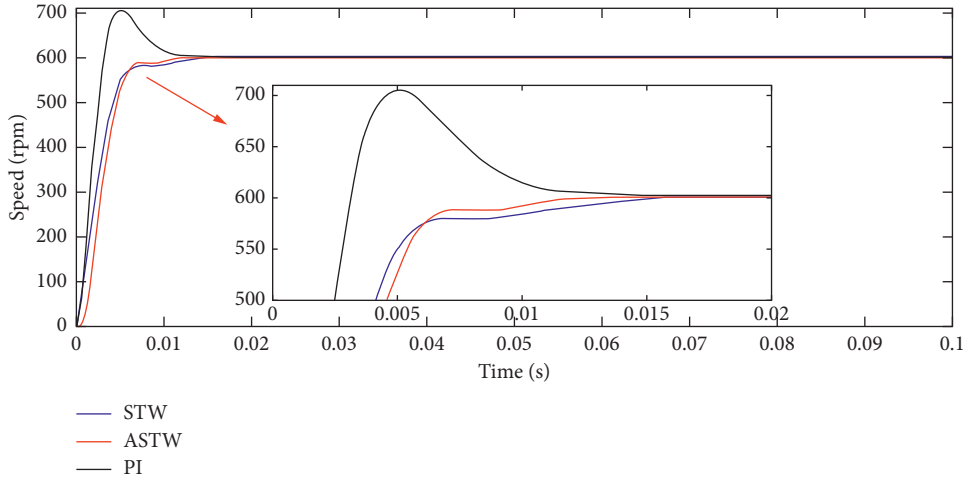


Figure 1: Comparison of the speed responses without load.

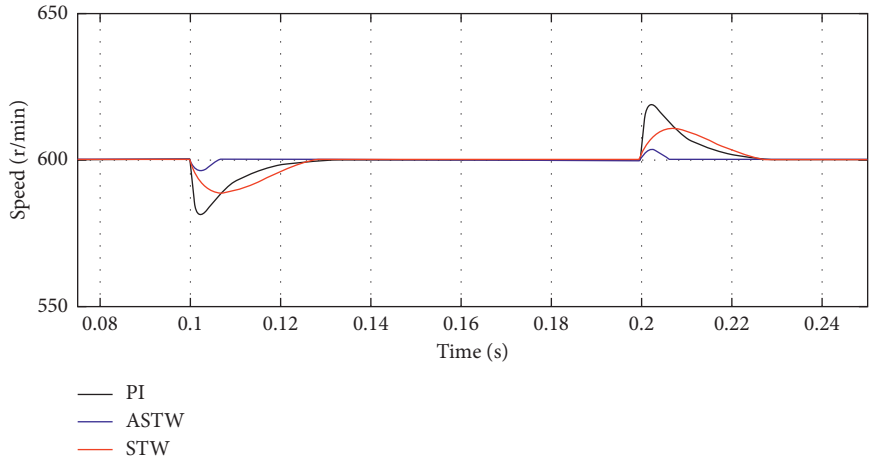


Figure 2: Comparison of the speed responses with load.

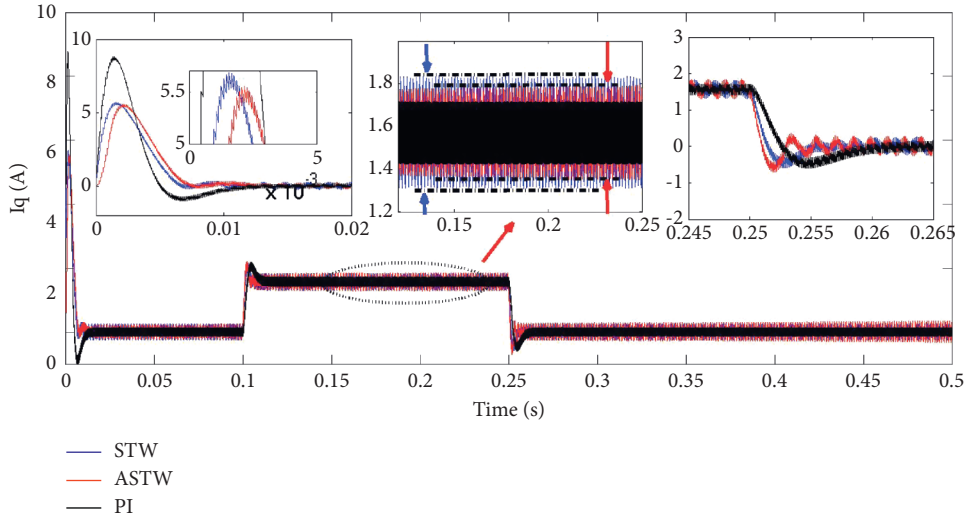


Figure 3: Comparison of the $q$-axis current responses.

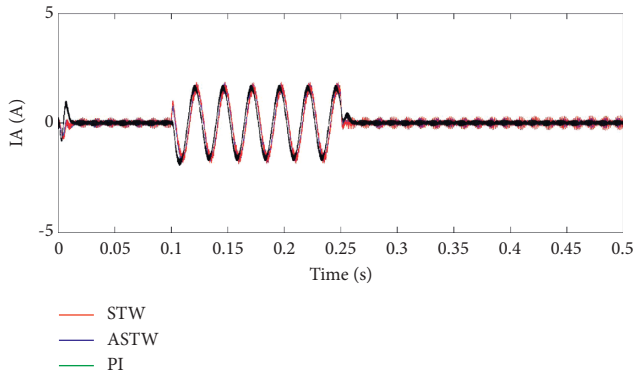


Figure 4: Comparison of the IA responses.

Table 2: Comparison of performance indices in PMSM simulation.

| Symbol | PI | STW | ASTW |
|---|---|---|---|
| Rise time $(t_r)$ | 0.0025 s | 0.015 s | 0.01 s |
| Adjusting time $(t_s)$ | 0.0125 s | 0 s | 0 s |
| Drop | 30$r$ | 20$r$ | 5$r$ |

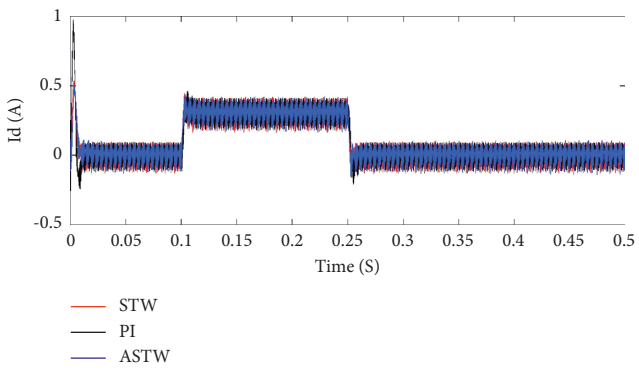


Figure 5: Comparison of the $d$-axis current responses.

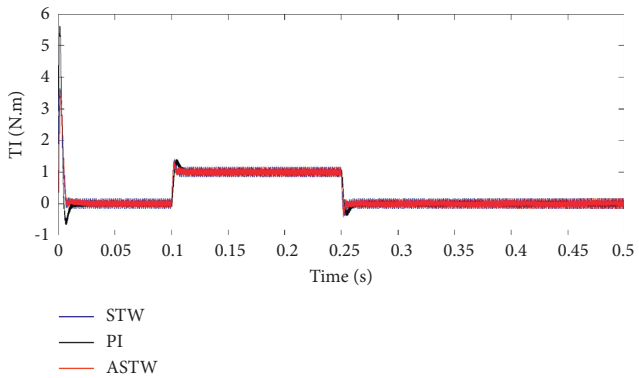


Figure 6: Comparison of the Tl.

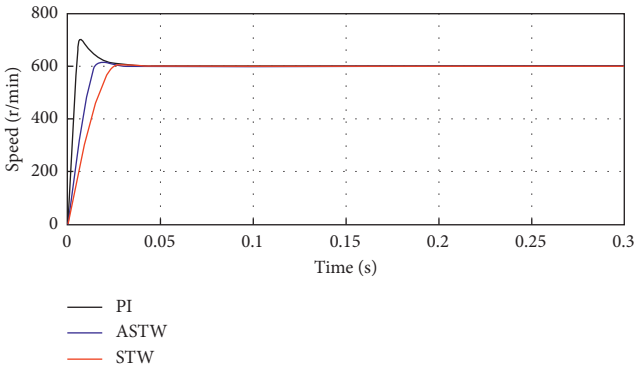


Figure 7: Comparative experimental diagram of PMSM motor speed in starting stage under PI, STW, and ASTW.

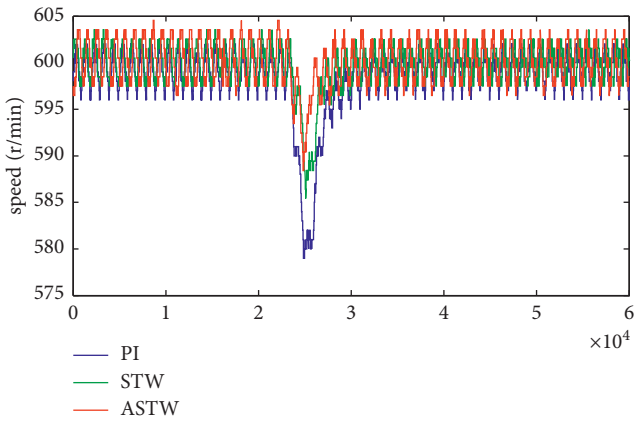


Figure 8: Comparative experimental diagram of PMSM motor speed in loading stage under PI, STW, and ASTW.

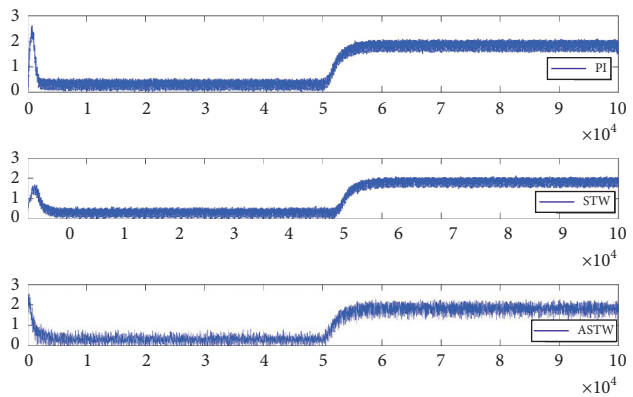


Figure 9: Comparative experimental diagram of $i_q$.

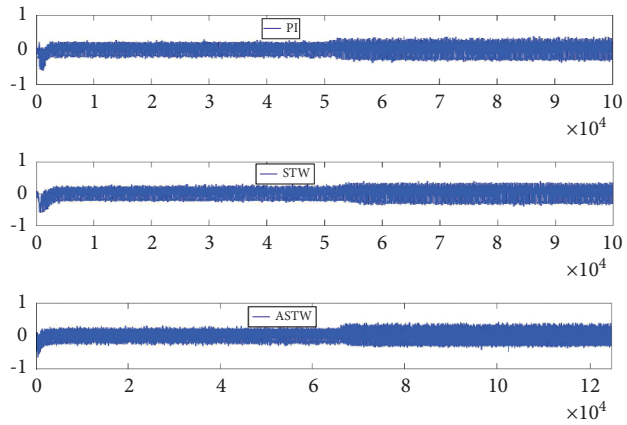


Figure 10: Comparative experimental diagram of $i_d$.

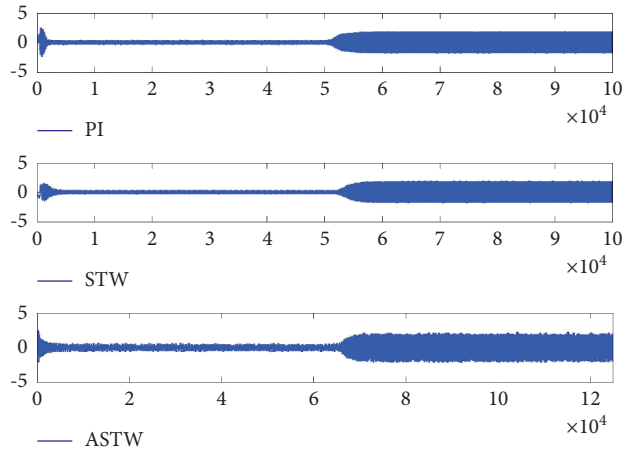


Figure 11: Comparative experimental diagram of $i_a$.

Table 3: Comparison of performance indices in PMSM experiment.

| Symbol | PI | STW | ASTW |
|---|---|---|---|
| Rise time ($t_r$) | 0.097 s | 0.143 s | 0.014 s |
| Adjusting time ($t_s$) | 0.114 s | 0.029 s | 0 s |
| Drop | 20$r$ | 14$r$ | 9$r$ |

responses in the startup phase and with load, respectively. A comparison of performance indices on the three methods is shown in Table 3.

## 5. Conclusions

This paper has developed a novel speed loop controller for the PMSM system. By combining the super-twisting algorithm with the adaptive law, the proposed speed controller has excellent robustness because it does not depend on the information of the lumped disturbance. It has also been proved that the signal of the lumped disturbance is bounded, and the speed error of the closed-loop system converges to zero at the mathematical level. Both simulation and experiment results are given to clearly confirm that the proposed speed regulator gives very remarkable speed-control performance without the information on the lumped disturbance.

## Data Availability

No data were used to support this study.

## Conflicts of Interest

The authors declare that they have no conflicts of interest.

## Acknowledgments

This study was supported by the Guiding Funds for Industrial Development of Suqian City under grant no. S201920.

## References

[1] B. Xu, L. Zhang, and W. Ji, "Improved non-singular fast terminal sliding mode control with disturbance observer for PMSM drives," *IEEE Transactions on Transportation Electrification*, p. 1, 2021.

[2] S. Li and Z. Liu, "Adaptive speed control for permanent-magnet synchronous motor system with variations of load inertia," *IEEE Transactions on Industrial Electronics*, vol. 56, no. 8, pp. 3050–3059, 2009.

[3] Q. Hou and S. Ding, "GPIO based super-twisting sliding mode control for PMSM," *IEEE Transactions on Circuits and Systems II: Express Briefs*, vol. 68, no. 2, pp. 747–751, 2021.

[4] X. Li, J. Shen, H. Akca, and R. Rakkiyappan, "LMI-based stability for singularly perturbed nonlinear impulsive differential systems with delays of small parameter," *Applied Mathematics and Computation*, vol. 250, pp. 798–804, 2015.

[5] Q. Hou, S. Ding, and X. Yu, "Composite super-twisting sliding mode control design for PMSM speed regulation problem based on a novel disturbance observer," *IEEE Transactions on Energy Conversion*, vol. 99, p. 1, 2020.

[6] S. Tong and H. X. Li, "Fuzzy adaptive sliding-mode control for MIMO nonlinear systems," *IEEE Transactions on Fuzzy Systems*, vol. 11, no. 3, pp. 354–360, 2003.

[7] L. Fang, S. Ding, J. H. Park, and L. Ma, "Adaptive fuzzy output-feedback control design for a class of p-norm stochastic nonlinear systems with output constraints," *IEEE Transactions on Circuits and Systems I: Regular Papers*, vol. 68, no. 6, pp. 2626–2638, 2021.

[8] S. Ding, W. X. Zheng, J. Sun, and J. Wang, "Second-order sliding-mode controller design and its implementation for buck converters," *IEEE Transactions on Industrial Informatics*, vol. 14, no. 5, pp. 1990–2000, 2018.

[9] L. Liu, W. X. Zheng, and S. Ding, "An adaptive SOSM controller design by using a sliding-mode-based filter and its application to buck converter," *IEEE Transactions on Circuits and Systems I: Regular Papers*, vol. 67, no. 7, pp. 2409–2418, 2020.

[10] Y. Luo, Y. Chen, H.-S. Ahn, and Y. Pi, "Fractional order robust control for cogging effect compensation in PMSM position servo systems: stability analysis and experiments," *Control Engineering Practice*, vol. 18, no. 9, pp. 1022–1036, 2010.

[11] X. Li, D. O'Regan, and H. Akca, "Global exponential stabilization of impulsive neural networks with unbounded continuously distributed delays," *IMA Journal of Applied Mathematics*, vol. 80, no. 1, pp. 85–99, 2015.

[12] N. Jin, X. Wang, and X. Wu, "Current sliding mode control with a load sliding mode observer for permanent magnet synchronous machines," *Journal of Power Electronics*, vol. 14, no. 1, pp. 105–114, 2014.

[13] D. Yang, X. Li, and J. Qiu, "Output tracking control of delayed switched systems via state-dependent switching and dynamic output feedback," *Nonlinear Analysis: Hybrid Systems*, vol. 32, pp. 294–305, 2019.

[14] S. Li, M. Zhou, and X. Yu, "Design and implementation of terminal sliding mode control method for PMSM speed regulation system," *IEEE Transactions on Industrial Informatics*, vol. 9, no. 4, pp. 1879–1891, 2013.

[15] D. Yang, X. Li, J. Shen, and Z. Zhou, "State-dependent switching control of delayed switched systems with stable and unstable modes," *Mathematical Methods in the Applied Sciences*, vol. 41, no. 16, pp. 6968–6983, 2018.

[16] K. Mei and S. Ding, "HOSM controller design with asymmetric output constraints," *Science China Information Sciences*, vol. 65, Article ID 189202, 2022.

[17] J. Yuan, S. Ding, and K. Mei, "Fixed-time SOSM controller design with output constraint," *Nonlinear Dynamics*, vol. 102, no. 3, pp. 1567–1583, 2020.

[18] S. Ding, B. Zhang, K. Mei, and J. H. Park, "Adaptive fuzzy SOSM controller design with output constraints," *IEEE Transactions on Fuzzy Systems*, p. 1, 2021.

[19] J. Hu, G. Sui, X. Lv, and X. Li, "Fixed-time control of delayed neural networks with impulsive perturbations," *Nonlinear Analysis: Modelling and Control*, vol. 23, no. 6, pp. 904–920, 2018.

[20] Y. Feng, X. Yu, and F. Han, "High-order terminal sliding-mode observer for parameter estimation of a permanent-magnet synchronous motor," *IEEE Transactions on Industrial Electronics*, vol. 60, no. 10, pp. 4272–4280, 2013.

[21] K. Mei and S. Ding, "Second-order sliding mode controller design subject to an upper-triangular structure," *IEEE Transactions on Systems, Man, and Cybernetics: Systems*, vol. 51, no. 1, pp. 497–507, 2021.

[22] Y. Shtessel, M. Taleb, and F. Plestan, "A novel adaptive-gain supertwisting sliding mode controller: methodology and application," *Automatica*, vol. 48, no. 5, pp. 759–769, 2012.

[23] E. Cruz-Zavala and J. A. Moreno, "Homogeneous high order sliding mode design: a Lyapunov approach," *Automatica*, vol. 80, pp. 232–238, 2017.

[24] V. Utkin, "Discussion aspects of high-order sliding mode control," *IEEE Transactions on Automatic Control*, vol. 61, no. 3, pp. 829–833, 2016.

[25] L. Feng, M. Deng, S. Xu, and D. Huang, "Speed regulation for PMSM drives based on a novel sliding mode controller," *IEEE Access*, vol. 8, pp. 63577–63584, 2020.

[26] H.-W. Chai, "Sliding mode control of PMSM based on robust differentiator," in *Proceedings of the 2010 Second International Conference on Computational Intelligence and Natural Computing*, pp. 37–40, Wuhan, China, September 2010.

[27] J. Ma, G. G. Zhu, and H. Schock, "Adaptive control of a pneumatic valve actuator for an internal combustion engine," *IEEE Transactions on Control Systems Technology*, vol. 19, no. 4, pp. 730–743, 2011.

[28] H. Lee and V. I. Utkin, "Chattering suppression methods in sliding mode control systems," *Annual Reviews in Control*, vol. 31, no. 2, pp. 179–188, 2007.

[29] A. C. Huang and Y. H. Chen, "Adaptive multiple-surface sliding control for nonautonomous systems with mismatched uncertainties," *Automatica*, vol. 40, no. 1, pp. 1939–1945, 2004.

[30] Y. Zuo, X. Zhu, L. Quan, C. Zhang, Y. Du, and Z. Xiang, "Active disturbance rejection controller for speed control of electrical drives using phase-locking loop observer," *IEEE Transactions on Industrial Electronics*, vol. 66, no. 3, pp. 1748–1759, 2018.